Neurobiology of Aging 112 (2022) 170–180

Contents lists available at ScienceDirect

Neurobiology of Aging

journal homepage: www.elsevier.com/locate/neuaging.org

White matter lesion load is associated with lower within- and greater between- network connectivity across older age

Karin Kantarovich[a], Laetitia Mwilambwe-Tshilobo[b], Sara Fernández-Cabello[c,d], Roni Setton[b], Giulia Baracchini[b], Amber W. Lockrow[b], R. Nathan Spreng[b,e,f,g,#,*], Gary R. Turner[a,#]

[a] York University, Department of Psychology, Toronto, Ontario, Canada
[b] Montreal Neurological Institute, Department of Neurology and Neurosurgery, McGill University, Montreal, Quebec, Canada
[c] NORMENT, Division of Mental Health and Addiction, Oslo University Hospital, Oslo, Norway
[d] Department of Psychology, University of Oslo, Oslo, Norway
[e] McConnell Brain Imaging Centre, McGill University, Montreal, Quebec, Canada
[f] Departments of Psychiatry and Psychology, McGill University, Montreal, Quebec, Canada
[g] Douglas Mental Health University Institute, Verdun, Quebec, Canada

ARTICLE INFO

Article history:
Received 29 July 2021
Revised 31 December 2021
Accepted 21 January 2022
Available online 31 January 2022

Keywords:
White matter hyperintensities
Resting-state functional connectivity
Aging
Brain networks
Multi-echo fMRI
BOLD dimensionality

ABSTRACT

White matter hyperintensities (WMH) are among the most prominent structural changes observed in older adulthood. These changes coincide with functional changes to the intrinsic network organization of the aging brain. Yet little is known about how WMH are associated with changes to the whole-brain functional connectome in normal aging. We used a lesion prediction algorithm to quantify WMH as well as resting-state multiecho functional magnetic resonance imaging to characterize resting-state functional connectivity in a cross-sectional sample of healthy older adults (N = 105, 60–83 years of age). In a multivariate analysis, we found that higher lesion load was associated with a global pattern of network dedifferentiation, marked by lower within- and greater between- network connectivity. Network specific changes included greater visual network integration and greater posterior-anterior connectivity. The relationship between WMH and resting-state functional connectivity was negatively associated with fluid IQ as well as Blood Oxygen Level Dependent signal dimensionality. Reduced functional network segregation is a widely observed pattern of age-related change. Our findings show that these functional changes are associated with the accumulation of WMH in older adulthood.

1. Introduction

White matter lesions are among the most pervasive structural brain changes occurring in later in life, with prevalence rates approaching 95% of adults over the age of 45 (de Leeuw et al., 2002; Habes et al., 2018; Vernooij et al., 2007). Lesions are typically indexed by the presence of white matter hyperintensities (WMH) on fluid-attenuated inversion recovery (FLAIR) magnetic resonance images (Debette & Markus, 2010; Kloppenborg et al., 2014; Prins & Scheltens, 2015). WMHs are associated with vascular and amyloid pathologies in older adults (Arfanakis, 2020; Walsh, 2020), and predict more rapid cognitive decline as well as earlier emergence of clinical syndromes, including Alzheimer's disease (Black et al., 2009; Sachdev et al., 2014; Vasquez & Zakzanis, 2015). Investigating how these structural brain changes impact brain function, and ultimately cognitive abilities, into older age is of increasing urgency in a rapidly aging population (World Health Organization, 2021).

Alterations in large-scale functional brain networks are also a hallmark of brain aging. Functional brain networks are observable during wakeful rest, in the absence of explicit task demands, and are characterized by low-frequency oscillations among spatially distributed brain regions that cohere to form the intrinsic functional network architecture of the brain (Biswal et al., 2010; Fox & Raichle, 2007; Yeo et al., 2011). These resting state brain networks are formed by Hebbian-like mechanisms and shaped by repeated patterns of co-activation (or inhibition) occurring across timescales from moments to decades (Stevens & Spreng, 2014). We have argued that changes to the network architecture of the aging

Co-senior authorship.
* Corresponding author at: Montreal Neurological Institute, 3801 University St. Montreal, Quebec, H3A 2B4, Canada, Tel.: 514-398-7268, fax: 514-398-8248.
E-mail address: nathan.spreng@gmail.com (R.N. Spreng).

0197-4580/$ – see front matter © 2022 Elsevier Inc. All rights reserved.
https://doi.org/10.1016/j.neurobiolaging.2022.01.005

brain parallels the shifting architecture of cognition in older adulthood (Spreng & Turner, 2019b), and there is growing evidence that alterations in resting state functional connectivity (RSFC) patterns are associated with age-related cognitive decline (Chan et al., 2014; Geerligs et al., 2014; Varangis et al., 2019; Stumme et al., 2020). Given the increasing prevalence of WMH in later life, we reasoned that these structural changes would be associated with alterations to the whole-brain intrinsic functional connectome in older adults.

There is preliminary evidence for such an association. White matter pathology was associated with altered RSFC among spatially distributed brain regions in a small healthy adult lifespan sample (De Marco et al., 2017). This study investigated compensatory neuroplastic changes, focusing only on positive associations between WMH, RSFC as well as grey matter volumes within a circumscribed set of brain regions and networks. Lesions within *a priori* defined white matter tracts have also been associated with RSFC between tract-specific brain regions, with differences observed in both direct and indirect functional connectivity (Langen et al., 2017). Similarly, white matter lesions in stroke and other neurological conditions have been associated with altered functional connections between brain regions (Fridriksson et al., 2013; Johnston et al., 2008; Nomura et al., 2013; Schonberg et al., 2006; Seghier et al., 2004; Song et al., 2014, and see Dey et al., 2016 for a review). Taken together, these findings suggest that age-related white matter changes may be associated with altered RSFC among large-scale brain networks in older adulthood. However, the impact of distributed WMH on the whole-brain functional connectome is unknown. Understanding these brain-wide structure-function associations can provide novel insights into the downstream impacts of WMH on brain function and ultimately how these functional shifts manifest as behavioral changes in later life (Spreng & Turner, 2019b).

Here we examined how age-related white matter changes, measured as WMH, were associated with the shifting architecture of the whole-brain functional connectome in typically aging older adults. We predicted that white matter lesion load in later life would be associated with patterns of age-related functional network dedifferentiation reported previously (Chan et al., 2014; Setton et al., 2022; see Damoiseaux, 2017 for a review). To test this prediction, we first quantified white matter lesion burden using a lesion prediction algorithm. For the RSFC analyses, we implemented 3 innovative approaches (Setton et al., 2022). First, a multi-echo functional magnetic resonance imaging (ME-fMRI) acquisition sequence was used to separate neural Blood Oxygen Level Dependent (BOLD) from non-neural (noise) components in the BOLD signal. Previous work has demonstrated that BOLD signal dimensionality decreases across the lifespan and has been related to large-scale network changes (Kundu et al., 2017; Setton et al., 2022). Further, ME-fMRI improves signal to noise ratios, particularly in areas of signal drop-out due to air-tissue interfaces or atrophic changes. Next, we used individually defined cortical parcellations to identify discrete person-specific functional brain regions across the cortical mantle, thereby reducing potential spatial distortions across subjects (Chong et al., 2017). Finally, we implemented multivariate, partial least squares (PLS, Misic & McIntosh, 2013) analysis to investigate whole-cortical patterns of RSFC associated with WMH in cognitively healthy older adults.

2. Material and methods

2.1. Participants

One hundred and five healthy older adults were included in this study (57% female; Mage = 68.35; age range: 60–83). See Table 1 for sample demographics. Data were drawn from a collaborative neuroimaging and neuropsychological data collection initiative at York University (n = 28) and Cornell University (n = 77). Participants were recruited from the community via flyers, word of mouth, advertisements (TV, radio, and print), a local community email list-serv, and research databases of participants who were previously involved in studies at York or Cornell. Standard inclusion and exclusion criteria were implemented to ensure all participants were healthy without evidence of neurological, psychiatric or other underlying medical conditions known to impact brain or cognitive functioning. Specifically, participants were screened to rule out individuals with acute or chronic psychiatric illness, those undergoing current or recent treatment with psychotropic medication, and those having recently experienced significant changes to health status. Participants were screened for depressive symptoms using the Geriatric Depression Scale (Yesavage et al., 1982). We administered the Mini-Mental State Examination (MMSE; Folstein et al., 1975) to rule out mild cognitive impairment or sub-clinical dementia. Participants with MMSE scores below 27/30 were excluded if NIH Toolbox fluid cognition scores (Gershon et al., 2013) also fell below an age-adjusted national percentile of 25%. All participants were right-handed with normal or corrected-to-normal vision. Procedures were administered in compliance with the Institutional Review Board at Cornell University and the Research Ethics Board at York University. From this sample, T2-FLAIR data of 125 older adults was available for analysis. Nine of these participants did not have enough components required for ME-ICA, and 2 participants had anatomical abnormalities. An additional 4 participants were excluded due to depression (n = 2) or low cognition (n = 2). As such, 110 healthy older adults met study criterion. One participant was excluded due to artifacts that precluded white matter segmentation. Four additional participants were excluded as multivariate outliers, which did not impact the results. Extended neuropsychological assessment was incomplete in 2 participants.

2.2. Behavioral assessment of neurocognitive functioning

Performance on measures of fluid intelligence (fluid IQ) and crystallized intelligence (crystallized IQ) was assessed to characterize the cognitive abilities of each participant. Assessments of fluid IQ and crystallized IQ were obtained using the Unadjusted Fluid Cognition and Crystallized Cognition Composite Scores from the National Institute of Health (NIH) Toolbox Cognition Battery (http://www.nihtoolbox.org). Higher scores are indicative of better performance.

2.3. Neuroimaging acquisition

2.3.1. MRI acquisition

Neuroimaging data were acquired from 2 sites with a 3T GE750 Discovery series MRI scanner and 32-channel head coil at the Cornell Magnetic Resonance Imaging Facility or on a 3T Siemens Tim Trio MRI scanner with a 32-channel head coil at the York University Neuroimaging Center in Toronto.

2.3.2. T2-FLAIR/white matter hyperintensities

T2-weighted FLAIR sequences were acquired at Cornell (TR = 12000 ms; TE = 95 ms; TI = 2712 ms; 160° flip angle; 42 slices of 1 × 1 × 3 mm; 2 m 36 s) and at York (TR = 12000 ms; TE = 95 ms; TI = 2759.4 ms; 160° flip angle; 44 slices of 0.8 × 0.8 × 3 mm; 3 m 38 s).

2.3.3. T1/anatomical

T1 anatomical scans at Cornell were acquired using a T1-weighted volumetric magnetization prepared rapid gradient echo

Table 1
Sample demographics

	n	%
Gender		
Female	60	57.10
Male	45	42.90
Race/Ethnicity		
White	94	89.52
Asian	3	0.03
Black	2	0.19
Hispanic	2	0.19
Other/Not Provided	4	0.04

Variable	n	Minimum	Maximum	Mean	SD
Age (years)	105	60	83	68.35	6.17
Education (years)	105	12	24	17.28	2.95
Raw Lesion Volume (mm^3)	105	23.00	28197.00	1670.66	3331.05
Total Intracranial Volume (mm^3)	105	1094150	2093480	1563410.70	188315.88
Total Lesion Volume (mm^3)	105	0.02	2.54	0.76	0.68
Number of Lesions	105	1	25	9.71	4.66
BOLD Dimensionality	105	10.5	32	18.11	4.48
Crystallized-IQ	104	112.63	153.95	136.07	10.54
Fluid-IQ	103	78.21	122.79	94.79	6.98

Note. Total Lesion Volume, Raw Lesion Volume divided by Total Intracranial Volume; SD, standard deviation. Total lesion volume and number of lesion values include winsorized observations.

sequence (TR = 2530 ms; TE = 3.4 ms; 7° flip angle; 1mm isotropic voxels, 176 slices, 5 m 25 s) with 2x acceleration with sensitivity encoding. At York, anatomical scans were acquired using a T1-weighted volumetric magnetization prepared rapid gradient echo sequence (TR=1900ms; TE = 2.52 ms; 9° flip angle; 1mm isotropic voxels, 192 slices, 4 m 26 s) with 2x acceleration and generalized auto calibrating partially parallel acquisition (GRAPPA) encoding at an iPAT acceleration factor of 2. While these acquisition parameters were aligned as closely as possible across sites, we cannot rule out that estimations in lesion volume may vary slightly due to marginal differences in scanner sequences. However, all analyses reported below include site as a covariate.

2.3.4. Resting-state functional MRI

Two 10 minutes 06 seconds resting-state runs were acquired using a multi-echo (ME) EPI sequence at Cornell University (TR = 3000 ms; TE_1 = 13.7ms, TE_2 = 30 ms, TE_3 = 47 ms; 83° flip angle; matrix size = 72 × 72; field of view (FOV) = 210 mm; 46 axial slices; 3 mm isotropic voxels; 204 volumes, 2.5x acceleration with sensitivity encoding) and York University(TR = 3000 ms; TE1 = 13.7 ms, TE2 = 30 ms, TE3 = 47 ms; 83° flip angle; matrix size = 64 × 64; FOV = 216 mm; 43 axial slices; 3.4 × 3.4 × 3 mm voxels; 200 volumes, 3x acceleration and GRAPPA encoding). Participants were instructed to lay still with their eyes open, breathing and blinking normally in the darkened scanner bay.

2.4. Image processing

2.4.1. T2-FLAIR/white matter lesion load

T2-FLAIR structural MRI sequences were used to evaluate WMH load volume and quantity. WMH were segmented by the lesion prediction algorithm (LPA; Schmidt, 2013, Chapter 6.1) as implemented in the Lesion Segmentation Toolbox (LST) version 2.0.15 (www.statistical-modelling.de/lst.html) for Statistical Parametric Mapping. As covariates for this model, a lesion belief map showing voxels that appear hyperintense on FLAIR images and that are likely to be part of the white matter was used (Schmidt et al., 2012). In addition, a spatial covariate that takes into account voxel specific changes in lesion probability was implemented. Parameters of this model fit are used to segment lesions in new images by providing an estimate for the lesion probability for each voxel. For the calculation of the lesion probability maps, T2-weighted FLAIR images were used. The resulting output was a probability lesion map in FLAIR space for each participant. Given that FLAIR images can be affected by artifacts such as cerebrospinal fluid pulsation, subject-specific anatomical masks were created using FSL tools (https://fsl.fmrib.ox.ac.uk/fsl/fslwiki/BIANCA) to exclude voxels that were not part of the white matter. T1 images were processed with FreeSurfer. The T1 high-resolution biased corrected images and dilated cerebrospinal fluid masks of each participant were used to create the anatomical masks. To ensure appropriate tissue classification, we masked each subject's lesion probability mask with a subject-specific exclusion mask, including WM and excluding GM, subcortical GM and cerebellum (See Supplementary Figure 1 for a sample mask and procedure for lesion number and volume extraction). The masks were then warped to each individual's native FLAIR space. Regions falling outside the mask were excluded from the probability lesion maps. Finally, the masked lesion probability maps were used to calculate the total lesion volumes (in units of cubic millimeters) and the total number of lesions for each participant (See Supplementary Table 1 for lobar-specific values). Each participant's raw total lesion volume was then divided by their estimated total intracranial volume (eTIV) in mm^3 to correct for head size. Final total lesion volume (TLV) and number of lesions data were converted to within-sample z-scores for subsequent analysis. The combination of total lesion volume and number of lesions is collectively referred to as "white matter lesion load".

The inferential procedure of PLS is based on resampling statistics (permutation testing), rather than GLM parametric methods; it does not make any assumptions about data normality. Further, PLS has been shown to be robust to skewed response distributions (see Cassel et al. 1999). Given this, we chose to report non-log transformed TLV and number of lesion values in the main text as these are veridical representations of the data. Further, there is evidence that log-transformations can possibly exacerbate skewness (Feng et al., 2014), and large sample sizes as we report here are considered robust to violations of the normality assumption (Ghasemi & Sahesiasl, 2012). However, we report all analyses with log-transformed total lesion volumes in Supplementary Materials (Section S3).

2.4.2. Functional MRI processing

Functional images were submitted to multi-echo independent components analysis (ME-ICA; version 3.2 beta; https://github.com/ME-ICA/me-ica; Kundu et al., 2012, 2013). ME-ICA relies on the TE-dependence model of BOLD signal to better approximate T2* in every voxel and differentiate BOLD signal from non-BOLD sources of noise. Prior to TE-dependent denoising, time series data were minimally pre-processed: the first 4 volumes were discarded, matrices were computed for de-obliquing, motion correction, and anatomical-functional coregistration, and each TE was brought into spatial alignment. Anatomical-functional coregistration was driven by the T2* map which delineates grey matter and cerebrospinal fluid compartments more precisely than raw EPI images (Kundu et al., 2017; Speck et al., 2001). This is a critical consideration in aging research given that structural changes, such as enlarged ventricles and greater subarachnoid space, blur the boundary between them. TEs were then optimally combined and de-noised.

Post-processing quality assessment was performed on the de-noised time series in native space to identify and exclude participants with unsuccessful coregistration, residual noise (in-scanner motion, or absolute displacement, in any direction $>$ 3 mm coupled with de-noised time series showing DVARS $>$1; Power et al., 2012), poor temporal signal to noise ratio (tSNR; $<$ 50), or fewer than 10 retained BOLD-like components. The de-noised ICA coefficient sets in native space, optimized for functional connectivity analyses (Kundu et al., 2013), were used in subsequent steps. We refer to these as multi-echo functional connectivity (MEFC) data. Computing functional connectivity with approximately independent coefficients rendered global signal regression unnecessary (Spreng et al., 2019). Critically, ME-ICA effectively removes distant dependent RSFC motion confounds from fMRI data (Power et al., 2018).

2.4.3. RSFC parcellation

Whole brain RSFC matrices were initialized with the 200-parcel Schaefer atlas (Schaefer et al., 2018), corresponding to 7 RSFC-defined networks (Yeo et al., 2011). Participant-specific functional connectomes were then computed with the Group Prior Individual Parcellation algorithm (GPIP; Chong et al., 2017; Mwilambwe-Tshilobo et al., 2019). To do so, MEFC data were mapped to a common cortical surface for each participant using FreeSurfer (Fischl, 2012). To maximize alignment between intensity gradients of structural and functional data (Greve & Fischl, 2009), MEFC data were first linearly registered to the T1-weighted image by run. The inverse of this registration was used to project the T1-weighted image to native space and resample the MEFC data onto a cortical surface (fsaverage5) with trilinear volume-to-surface interpolation. Once on the surface, runs were concatenated and MEFC data at each vertex were normalized to zero mean and unit variance. We generated subject-specific functional parcellations to examine individual differences in functional brain network organization with a group sparsity prior approach (GPIP; Chong et al., 2017). Relative to group-based parcellations, GPIP has been shown to improve homogeneity of resting activity within parcels and delineation between regions of functional specialization (Chong et al., 2017). This approach therefore enables a more accurate estimation of subject-specific individual functional areas (Chong et al., 2017), and may be better suited to detect RSFC associations with behavior (e.g. Kong et al., 2021; Mwilambwe-Tshilobo et al., 2019). We extracted the resulting MEFC data from each parcel and computed the product-moment correlation between each pair, resulting in a 200 $\times$ 200 functional connectivity matrix (Ge et al., 2017). The canonical Fisher's r-to-z transformation was then applied to account for variation in MEFC data degrees of freedom, or the number of de-noised ICA coefficients, across individuals (Kundu et al., 2013).

2.4.3.1. BOLD dimensionality. A unique advantage of ME-fMRI and the MEICA processing framework is that BOLD- and non-BOLD-like signals can be separated into independent components. BOLD dimensionality may then be examined (Kundu et al., 2018; Setton et al., 2022), which is the number of BOLD components identified in the ME-fMRI timeseries. In the current study, BOLD dimensionality was computed for each participant by averaging the number of BOLD components retained from each run.

2.5. Data analysis

All product-moment and partial correlations were conducted with SPSS version 27 with a 95% Confidence Interval (CI) based on 500 bootstrap samples and statistical significance set at $p <$ 0.05. All partial correlation analyses controlled for the effects of site for data collection, participant age, gender, and years of education. Given prior literature characterizing associations between white matter lesion load, age, and cognition (Cook et al., 2004; Gunning-Dixon & Raz, 2000; Kramer et al., 2007, Raz et al., 2005; Vernooij et al., 2007), *a priori* correlations between these variables were 1-tailed. All subsequent statistical tests were 2-tailed.

2.5.1. Partial least squares

Behavioural Partial Least Squares (bPLS) was performed to identify RSFC patterns associated with individual differences in white matter lesion load (TLV and number of lesions; McIntosh & Lobaugh, 2004; McIntosh & Misic, 2013). PLS is a data-driven, multivariate statistical technique that allows for concurrent replication of previous RSFC patterns and explorative investigation of relationships outside of previously examined networks. For this reason, it was considered the preferred method of analysis for this study. In this study white matter lesion load values were treated as behavioral variables. 500 Permutation tests were used to evaluate the significance of the pattern of RSFC captured by a given latent variable (LV), while 500 bootstrap samples were used to determine its reliability. Large 'bootstrap ratios' (BSRs) correspond to brain functional connections and behaviors that have large weights and narrow confidence intervals. BSRs are equivalent to z-scores if the sampling distribution is approximately unit normal (Efron & Tibshirani, 1986). Brain network connections were considered reliable if the absolute value of the BSR exceeded $\pm$1.98 (approximately $p <$ 0.05) and were visualized using BrainNet Viewer (Xia et al., 2013) with a BSR threshold of $\pm$4 ($p <$ 0.0001) for visualization.

We next determined the network-level functional connectivity associations of the visual network (VIS), somatomotor network (SOM), dorsal attention network (DAN), ventral attention network (VAN), limbic network (LIM), frontoparietal control network (FPN), and default network (DN), with white matter lesion load. Within- and between- network-level contributions for the derived connectivity pattern were examined following Mwilambwe-Tshilobo et al., (2019). Positive and negatively weighted adjacency matrices were binarized with BSR values of $\pm$1.98. The network-level functional connectivity contributions were quantified by averaging the weights of all connections in a given network, generating a 7 $\times$ 7 matrix, and performing 500 permutation tests against a null sampling distribution for network assignment and connectivity patterns (Shafiei et al., 2019).

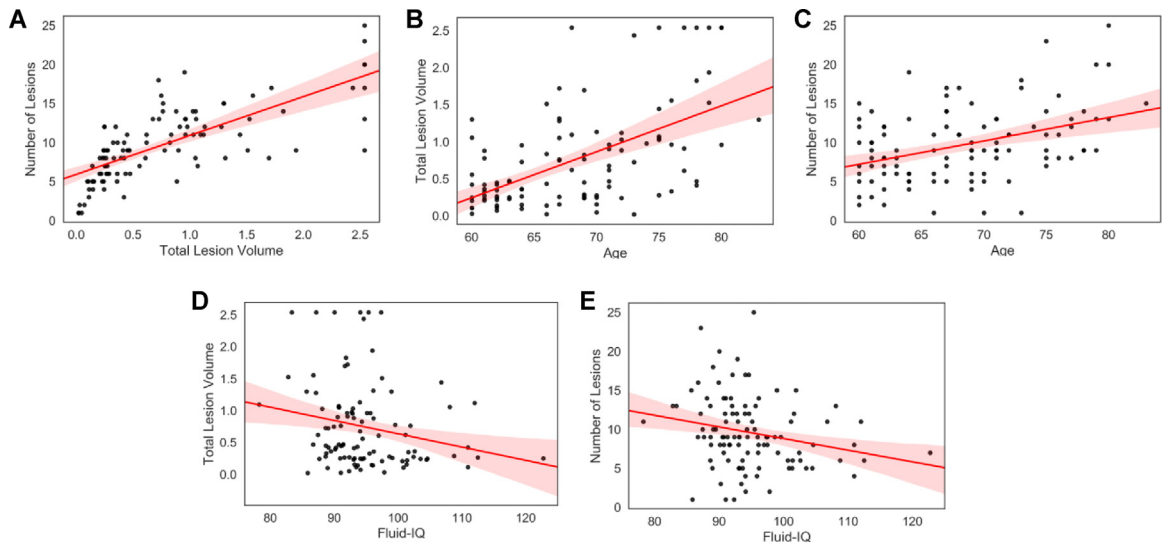

Fig. 1. Associations with white matter lesion load. (A) Total lesion volume is associated with number of lesions. Increasing age is associated with (B) Total lesion volume, and, (C) Number of lesions. Fluid-IQ is negatively associated with (D) Total lesion volume, and, (E) Number of lesions. Total lesion volume is corrected for intracranial volume and converted to standard units (z-score). Red shading represents 95% CI. (For interpretation of the references to color in this figure legend, the reader is referred to the Web version of this article.)

6. Results

6.1. Data analysis procedure

In a sample of healthy older adults, we characterized white matter lesion load, indexed by total lesion volume and number of lesions. We then examined the validity of these indices to confirm that estimates of white matter lesion load in our sample demonstrated patterns previously established in the literature (Cook et al., 2004; Gunning-Dixon & Raz, 2000; Kramer et al., 2007, Raz et al., 2005; Vernooij et al., 2007). This was accomplished by examining white matter lesion load associations with age and cognition. We then used a multivariate data-driven analytical model to investigate RSFC patterns associated with individual variability in white matter lesion load . Next, we extracted the metric of BOLD dimensionality (i.e., the number of BOLD components emerging from ME-ICA), which has been used a marker of functional network differentiation in younger (Kundu et al., 2018) and older (Setton et al., 2022) adults. We then examined how the relationship between white matter lesion load and RSFC was associated with cognition and BOLD dimensionality in our typically aging sample.

6.2. White matter lesion load

Consistent with expectations, total lesion volume and number of lesions were positively correlated ($r(103) = .730$, $p < 0.001$, CI: 0.60, 0.83; Fig. 1A). White matter lesion load was then examined for its associations with age and cognitive performance. Both total lesion volume and number of lesions were positively correlated with age ($r(103) = .562$, $p < 0.001$, CI: 0.42, 0.68; $r(103) = 0.398$, $p < 0.001$, CI: 0.23, 0.55, respectively; Fig. 1B–C). Both total lesion volume and number of lesions were negatively associated with fluid IQ ($r(101) = -.220$, $p = 0.013$, CI: -0.36, -0.05); $r(101) = -.227$, $p = 0.011$, CI: -0.37, -0.07, respectively; Fig. 1D–E). The associations between white matter lesion load and fluid IQ held when controlling for site, gender, age and education (total lesion volume: $pr(97) = -0.179$, $p = 0.038$, CI: -0.34, 0.03); number of lesions: $pr(97) = -.017$, $p = 0.046$, CI:-0.32, -0.02). There were no significant relationships found between indices of white matter lesion load and crystallized IQ.

6.3. Cortical RSFC and white matter lesion load

We examined the relationship between white matter lesion load and cortical inter-regional RSFC. PLS identified a significant pattern of connectivity (permuted $p = 0.034$, Fig. 2A) that was reliably associated with both total lesion volume and number of lesions (total lesion volume: $r = 0.67$, CI: 0.67, 0.84; number of lesions: $r = 0.67$, CI: 0.65, 0.83; Fig. 2B). The associations remained significant when controlling for site, age, gender, and years of education for total lesion volume ($pr(99) = .54$; $p < 0.001$, CI: 0.41, 0.65) and number of lesions ($pr(99) = .43$; $p < 0.001$, CI: 0.26, 0.36). White matter lesion load is associated with both lower and higher levels of inter-regional RSFC across the connectome (Fig. 2A).

When examining network level effects of white matter lesion load, we found systematic differences in within- and between- network connectivity patterns (Fig. 2C). White matter lesion load was predominantly associated with lower within-network connectivity in the SOM, DAN, VAN, LIM, and DN. Lesion load was also associated with lower connectivity between the SOM and VAN; LIM and SOM, and LIM and DN.

In addition to lower levels of RSFC associated with white matter lesion load, increases in RSFC were also observed. White matter lesion load was associated with greater visual network connectivity, both within this system and between the visual network to the DN, FPN, LIM, and VAN. Higher lesion load was also associated with greater between-network connectivity for the SOM to FPN, and VAN to DN.

The most robust and reliable inter-regional connections (i.e., those with BSR exceeding ±4.0; approximately $p < 0.0001$) associated with white matter lesion load are depicted in Fig. 2D. Greater white matter lesion load was associated with lower RSFC between contralateral regions, which form many within-network connections (Fig. 2D - blue). Higher white matter lesion load was associated with greater intra- and inter- hemispheric anterior-posterior connectivity, primarily comprising connectivity between anterior regions and the visual system (Fig. 2D - red).

The brain connectivity score is a composite score representing the extent to which each participant expresses the group RSFC matrix association with white matter lesion load. Controlling for age,

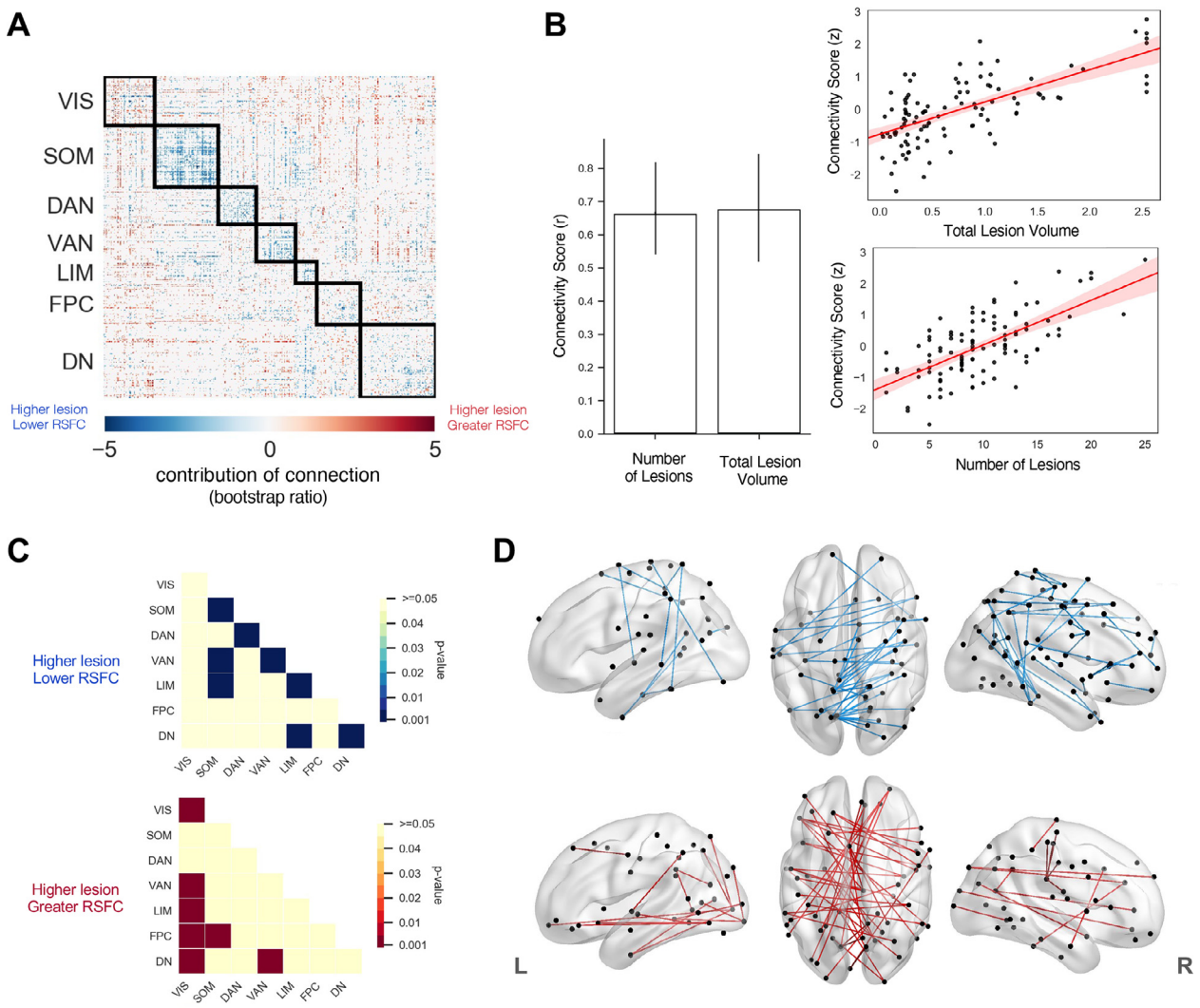

Fig. 2. Relationship between white matter lesion load and RSFC (A) The correlation matrix of reliable pairwise connections associated with number of lesions and total lesion volume (BSR magnitude ±1.98, $p < 0.05$, connections). (B) Bootstrapped correlations and scatterplots depict the relationship between connectivity scores and white matter lesion load. Red shading represents 95% CI. (C) Network level effects on the relationship between within- and between- network connectivity with white matter lesion load (D) Highest magnitude and reliable inter-regional connections associated with white matter lesion load (Bootstrap ratio (BSR) magnitude ±4, $p < 0.0001$, connections). Blue lines depicts lower connectivity with white matter lesion load. Red lines depict greater connectivity with white matter lesion load. Lateral views are within hemisphere. Dorsal view depicts between hemisphere. Nodes that are not connected by edges on lateral surfaces indicate cross-hemisphere connections. Abbreviations: VIS, visual; SOM, somatomotor; DAN, dorsal attention; VAN, ventral attention, LIM, limbic, FPN, frontoparietal network; DN, default network. Total lesion volume is adjusted for intracranial volume. (For interpretation of the references to color in this figure legend, the reader is referred to the Web version of this article.)

gender, and years of education and site, this connectivity score approached significance for its association with fluid IQ ($pr(97) = -.189$, $p = 0.061$, CI: -0.39 to 0.05). For associations with individual tasks comprising the NIH fluid cognition score, see Supplementary Tables 2 and 3. No association with crystallized IQ was observed.

6.4. BOLD dimensionality

Finally, we conducted an exploratory analysis of BOLD dimensionality's association with aging, white matter lesion load, and the brain connectivity scores identified above (which convey the relationship between RSFC and white matter lesion load across subjects). BOLD dimensionality was lower with advancing age ($r(103) = -0.243$, $p = 0.012$, CI: -0.44, -0.06; Fig. 3A). BOLD dimensionality was negatively associated with total lesion volume ($r(103) = -0.300$, $p = 0.002$, CI: -0.43, -0.14; Fig. 3B), and number of lesions ($r(103) = -0.246$, $p = 0.011$, CI: -0.41, -0.08; Fig. 3C). However, when controlling for site, age, gender, and years of education, BOLD dimensionality associations with indices of white matter load were no longer significant (total lesion volume: $pr(99) = -0.138$, $p = 0.169$, CI: -0.29, -0.05; number of lesions: $pr(99) = -0.111$, $p = 0.268$, CI: -0.29, -0.09). Critically, BOLD dimensionality showed a negative linear association with the brain connectivity scores, ($r(103) = -0.603$, $p < 0.001$, CI: -0.72, -0.47; Fig. 3D), and this association remained significant when controlling for site, age, gender, and years of education ($pr(99) = -.464$, $p < 0.001$, CI: -0.66, -0.20). These results show that the association between RSFC patterns and individual variability in white matter lesion load is related to BOLD dimensionality.

7. Discussion

We investigated whether white matter lesion load in typically-aging older adults was associated with the functional network organization of the brain. Consistent with predictions, lesion load was positively associated with age and negatively associated with

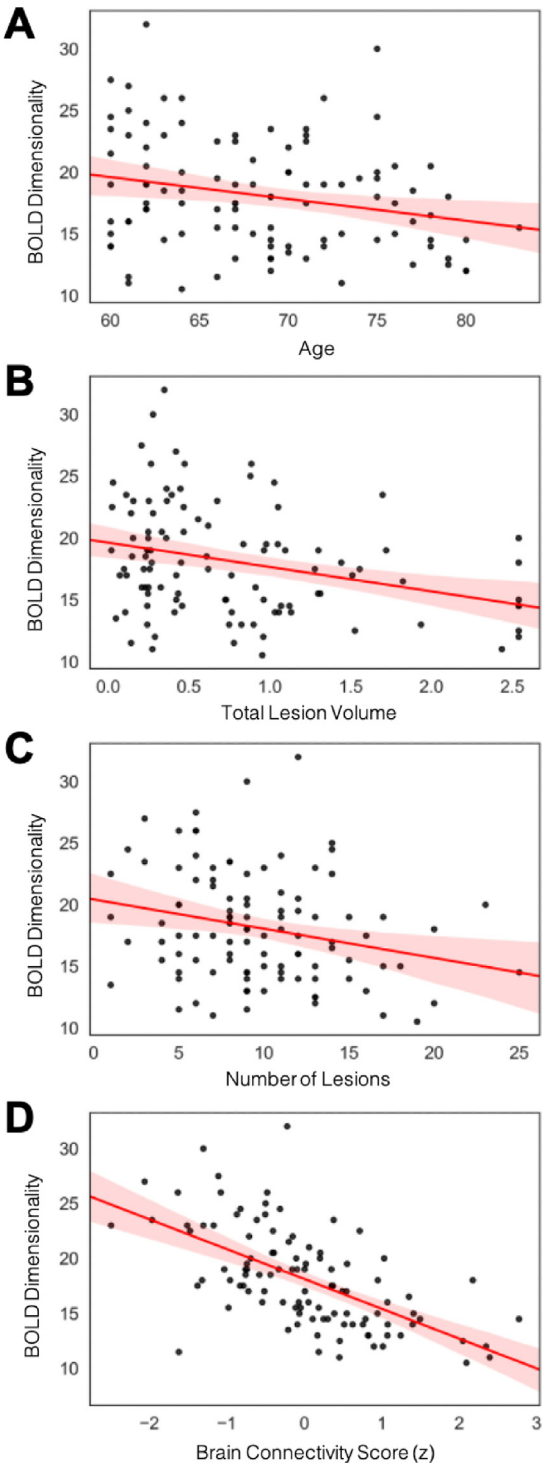

Fig. 3. BOLD dimensionality associations. (A) BOLD dimensionality declines with advancing age. BOLD dimensionality is negatively associated with (B) Total lesion volume, and (C) Number of lesions. (D) BOLD dimensionality shows a negative linear association with the relationship between RSFC and white matter lesion load. Red shading represents 95% CI. (For interpretation of the references to color in this figure legend, the reader is referred to the Web version of this article.)

fluid cognition. RSFC across the cortical connectome was associated with individual variability in white matter lesion load. Greater lesion load was associated with lower within-network connectivity and a pattern of predominantly higher connectivity between-networks, suggesting that damage to white matter pathways is associated with greater network dedifferentiation in older adulthood. Further, the expression of this WMH-RSFC pattern was associated with lower fluid IQ. Finally, in an exploratory analysis we observed that lower BOLD dimensionality (i.e., the number of non-noise BOLD components within resting-state ME-fMRI data), was associated with greater expression of this WMH-RSFC dedifferentiated network pattern. Together, these findings demonstrate that WMH are associated with significant alterations in the functional network architecture of the aging brain.

7.1. White matter lesion load and neurocognitive functioning

Our sample was a typically aging cohort of older adults and expressed no signs of an emergent clinical syndrome or cognitive impairment. Nonetheless, all older adults in this study displayed evidence of at least one WHM on FLAIR imaging. These findings provide strong support for concerns that cerebrovascular changes in later life, associated with WMH, may constitute an emerging public health priority. WMHs may be clinically 'silent', yet they are among the strongest predictors of major stroke, and can lead to more rapid cognitive decline when co-morbid with Alzheimer's disease pathology (Black et al., 2009; Sachdev et al., 2014; Vasquez & Zakzanis, 2015 and see Dey et al., for a review). Indeed, the presence of cerebral small vessel disease, including atherosclerosis, deep white matter lesions, or subcortical lacunar infarcts, is strongly associated with Alzheimer's disease onset (Yarchoan et al., 2012) and a nearly 2-fold increase in dementia risk (Snowdon et al., 1997). Consistent with these findings, chronological age is the primary predictor of the prevalence and degree of WMH (De Leeuw et al., 2001; Kennedy & Raz, 2015). Cross-sectional and longitudinal studies have revealed substantial white matter changes in normal aging, with volume loss estimated as high as 3 cm^3 per year (Resnick et al., 2003; Spreng & Turner, 2019b for a review). Declines in white matter volume and increases in WMH may also follow a curvilinear trajectory with more rapid changes occurring in the oldest old (Yang et al., 2016).

Further, these changes have direct impact on behavior as WMH has been linked to age-related cognitive decline, with higher lesion loads associated with poorer performance on complex cognitive tasks (Benson et al., 2018; Prins & Scheltens, 2015; Wirth et al., 2013; Quandt et al., 2020). Again, our findings are consistent with these reports, with white matter lesion load showing a robust, negative association with fluid cognition. The impact of white matter lesions on complex cognitive abilities is perhaps unsurprising. The prefrontal cortex, via its connections to other brain regions, is implicated in these higher order cognitive abilities and is selectively vulnerable to white matter pathology in older adulthood (Raz et al., 2005; Spreng & Turner, 2019b for review). The prevalence of white mater lesions across our healthy aging sample was universal, increased with age, and predicted lower fluid IQ. A critical question is whether and how these structural changes intersect with changes to functional brain networks, and how these associations may potentiate cognitive decline or promote resilience in later life.

7.2. White matter lesion load is associated with whole-brain RSFC

A reliable pattern emerged associating cortical RSFC with the number and total volume of white matter lesions. Broadly, this pattern was consistent with our predictions of a dedifferentiated network architecture, comprising lower within- and higher between- network RSFC. We observed a similar connectivity pattern in this cohort of older adults compared to younger adults in a cross-sectional study of the functional architecture of the brain (Setton et al., 2022). Here we provide novel evidence that this pattern of network dedifferentiation is positively associated with

white matter lesion load. While our cross-sectional study design does not allow us to evaluate within-subject changes, based on these findings we predict that the occurrence of white matter lesions may accelerate and steepen the trajectory of RSFC network dedifferentiation over the course of late-life development.

Further, clinical studies investigating white matter pathology of various etiologies (e.g., Multiple Sclerosis, Mild Cognitive Impairment, and Alzheimer's disease) have demonstrated associations with global alterations in neuronal activity (Sbardella et al., 2015; Soares et al., 2021; Zhou et al., 2015). Task-based fMRI studies of healthy older adults have also demonstrated distributed changes in functional activation patterns with increasing lesion load (Griebe et al., 2014) and this has been associated with tract-specific changes involving both direct and indirect functional connections (Langen et al., 2017). Here we demonstrate that white matter lesions result in altered functional connectivity extending well beyond local circuits, with impacts measurable across the whole functional connectome.

Finally, we observed that this pattern of WMH-RSFC was negatively associated with lower fluid IQ. No associations were observed with crystalized IQ. While preliminary, these cognitive findings suggest that the global pattern of WMH-RSFC associations observed here are specifically related to lower capacity for fast and flexible thinking, in the context of preserved crystalized cognition. These results provide additional support for our model linking the shifting architectures of brain and cognitive functioning in older adulthood (Spreng & Turner, 2019b).

7.3. White matter lesion load is associated with network-specific changes in RSFC

Our results suggest that the accumulation of white matter damage in late life development is associated with large-scale reorganization of intrinsic functional brain networks. Specifically, greater white matter pathology was associated with lower connectivity within nearly all the canonical resting-state networks investigated here, with the notable exception of the visual and frontoparietal control networks. In contrast, higher white matter lesion load was associated with increased between-network connectivity, particularly involving connections of the primary visual and somatosensory cortices to higher order association networks including frontoparietal control, default and ventral attention ("salience") networks. This extends our recent work demonstrating similar patterns of altered functional connectivity from younger to older adulthood (Setton et al., 2022), suggesting that the presence of white matter pathology may hasten these changes.

Recent reports have suggested that functional connectivity in response to the accumulation of WMH may reflect compensatory reorganization within specific neural circuits (Benson et al., 2018; De Marco et al., 2017). However, the current findings suggest that functional brain differences associated with global WMH values show reliable widespread network effects between spatially distributed brain regions spanning almost the entirety of the cortical mantle. This generalized pattern is not consistent with a more circumscribed, circuit-level, compensatory functional reorganization account. A shift from within- to greater between- network connectivity, or reduced network segregation, underpinned by the accumulation of white matter pathology with age, may reduce fluid cognitive resources. While we do not provide direct evidence here, reduced within- and increased between- network connectivity results in a dedifferentiated network architecture that has been associated with age-related cognitive decline in previous reports (Betzel et al., 2014; Chan et al., 2014; Geerligs et al., 2015; Malagurski et al., 2020; Strumme et al., 2020). We posit that structural disruptions imposed by WMH promote the collapse of a more efficient and modular network architecture present in younger adulthood (Bullmore et al., 2009), leading to network dedifferentiation and neurocognitive decline in later life.

While network dedifferentiation was the most prominent and generalized pattern of functional reorganization observed here, several other patterns of altered RSFC also emerged. Functional connectivity declined within most networks; however, the visual network demonstrated the opposite trend. White matter lesion load was associated with higher connectivity among brain regions within this network. We also note that the average number of lesions in occipital regions is relatively high given its size, compared to other lobes (Supplementary Table 1). While interpretations of this unexpected positive association between WMH and functional connectivity within the visual network would be purely speculative, we suggest that exploring these structural-functional associations within visual cortices would be an interesting area for future research.

Connectivity between the visual network and other networks was also associated with higher lesion load. We have reported greater integration of unimodal visual cortices with transmodal association networks in this cohort (Setton et al., 2022). Visual network integration into the larger connectome has now been replicated across several aging studies (Bethlehem et al., 2020; Geerligs et al., 2015; Stumme et al., 2020). Greater integration of visual brain regions with transmodal networks, implicated in top-down control, may reflect greater demands for top-down modulation of visual association cortices in the context of age-related declines in the fidelity of sensory signaling (Setton et al., 2022). The data here suggest that this requirement for greater control resources may be heightened in the context of greater white matter lesion burden.

Another notable pattern emerged from the whole-brain RSFC analyses, suggesting that greater white matter lesion load is associated with an altered spatial topography of RSFC. Higher lesion load was associated with greater connectivity between anterior and posterior regions and lower connectivity among posterior regions (Figure 2, panel D). This pattern was unexpected as long-range connectivity changes are difficult to isolate in RSFC studies of older adults due to the amplification of motion-related artifacts (Power et al., 2012). Our ME-fMRI acquisition sequence and ME-ICA denoising protocol enabled us to isolate BOLD from noise (including motion) components, enhancing our ability to detect changes in these longer-range connections (Power et al., 2018). As we did not pose any specific spatial predictions, interpretations of this pattern are speculative. However, greater anterior-posterior connectivity in the context of higher white matter lesion load would be consistent with several prominent theories of neurocognitive aging; the Posterior to Anterior Shift in Aging (Davis et al., 2008) or the Compensatory Recruitment of Neural Circuits Hypothesis (Reuter-Lorenz & Cappell, 2008). Both theories posit that declining sensory functioning imposes greater demands on higher-order attention and control processes mediated by frontal brain regions. The greater anterior-posterior connectivity pattern observed here may reflect a generalized increase in top-down attentional demands necessary to sharpen sensorineural representations as lesion load accumulates (Gazzaley et al., 2005; Turner & D'Esposito, 2011 for a review of this neuromodulatory account).

7.4. BOLD dimensionality, white matter lesion load and RSFC

By implementing an ME-fMRI and ME-ICA data acquisition and analysis protocol, we were able to conduct an exploratory analysis to measure individual differences in BOLD dimensionality. This novel metric, associated with network integration and dedifferentiation (Kundu et al., 2017), was examined for its relationship with

lesion load and RSFC patterns. Chronological age is a predictor of BOLD dimensionality, which declines from adolescence to early adulthood (Kundu et al, 2018) and continues to decline into older age (Setton et al., 2022). Here we report that BOLD dimensionality was associated with both of our measures of white matter lesion load, however, these associations were not significant when relevant covariates were included in the model. In contrast, BOLD dimensionality was robustly and reliably correlated with the connectivity pattern that emerged from the WMH-RSFC analysis. Greater expression of this WMH-RSFC pattern was associated with lower dimensionality in the BOLD signal. As such, we consider this as preliminary evidence that white matter integrity may contribute to changes in BOLD signal dimensionality into older adulthood. We interpret this finding as further support for our inference that the accumulation of white matter pathology may promote a dedifferentiated intrinsic network architecture in later life.

7.5. Limitations and future directions

There were several limitations to our study that will be important to address in future research. The cross-sectional nature of this study limits our ability to infer directionality and conclude with confidence that WMH lead to functional network reorganization, though the reverse is biologically unlikely. Furthermore, we acknowledge that in addition to WMH, other age-related neurobiological changes not accounted for in this study (e.g., grey matter loss, metabolic changes) are likely to contribute to changes in functional connectivity that we report here (Esiri, 2007). Sufficiently-powered longitudinal investigations are required to confirm the nature of these relationships.

In addition to acceleration of age-related white matter loss reported in the oldest old (Yang et al., 2016), a non-linear trajectory of functional network connectivity across different stages of older-adulthood has been reported in the longitudinal literature (Ng et al., 2016; Staffaroni et al., 2018). Future work that samples across the older adult age-cohort (80+) would further illuminate structure-function associations in healthy aging and could provide additional insights regarding when these interactions begin to manifest in measurable cognitive changes.

Finally, while the focus of the current study was to characterize global network changes in relation to age-related white matter pathology, specific regional changes were observed (see Supplementary Table 1 in Supplementary Materials) and would benefit from further exploration to investigate whether the network-related findings we report are influenced by specific spatial distributions of white matter lesions. However, given the variability in spatial distributions, such investigations will require large sample sizes to detect reliable associations.

8. Conclusion

Adopting several methodological and analytic innovations, we comprehensively characterized the global patterns of RSFC associated with WMH in cognitively normal older adults, advancing our understanding of these function-structure associations in this population. Older adulthood is associated with an increasing number and volume of white matter lesions. Accumulating lesion load alters RSFC patterns across the cortex. Greater white matter lesion load is associated with a dedifferentiated, and likely maladaptive, network architecture to support complex cognitive functioning in later life. In contrast, higher lesion load is also associated with greater visual network integration and anterior-posterior connectivity that has been associated with compensatory functional reorganization in previous work. Taken together these findings suggest that while clinically silent, white matter lesions may serve as an accelerant, hastening functional network changes in later life.

Credit author statement

Karin Kantarovich: Conceptualization, Formal analysis, Writing - Original Draft, Review & Editing, Visualization; Laetitia Mwilambwe-Tshilobo: Data Curation, Methodology, Resources, Writing - Review & Editing; -Cabello: Formal analysis, Resources, Software, Writing - Review & Editing; Roni Setton: Data Curation, Methodology, Resources, Writing - Review & Editing; Giulia Baracchini: Formal analysis, Software, Writing - Review & Editing; Amber W. Lockrow: Investigation, Data Curation, Writing - Review & Editing; R. Nathan Spreng: Conceptualization, Methodology, Writing - Original Draft, Review & Editing, Supervision, Project administration, Funding acquisition; Gary R. Turner: Conceptualization, 31 Methodology, Writing - Original Draft, Review & Editing, Supervision, Project administration, Funding acquisition

Disclosure statement

The authors declare that they have no conflict of interest.

Acknowledgements

This project was supported in part by grants to RNS from the Canadian Institute of Health Research and NIH (1S10RR025145) and to G.R.T from the Natural Sciences and Engineering Research Council of Canada (Discovery Grant).

Supplementary materials

Supplementary material associated with this article can be found, in the online version, at doi:10.1016/j.neurobiolaging.2022.01.005.

References

Arfanakis, K., Evia, A.M., Leurgans, S.E., Cardoso, L.F., Kulkarni, A., Alqam, N., Lopes, L.F., Vieira, D., Bennett, D.A., Schneider, J.A., 2020. Neuropathologic correlates of white matter hyperintensities in a community-based cohort of older adults. J. Alzheimer's Dis. 73 (1), 333–345.

Biswal, B.B., Mennes, M., Zuo, X.N., Gohel, S., Kelly, C., Smith, S.M., Beckmann, C.F., Adelstein, J.S., Buckner, R.L., Colcombe, S. and Dogonowski, A.M. (2010). Toward discovery science of human brain function. *Proceedings of the National Acad. Sci.*, 107(10), 4734-4739.

Benson, G., Hildebrandt, A., Lange, C., Schwarz, C., Kobe, T., Sommer, W., Floel, A., Wirth, M., 2018. Functional connectivity in cognitive control networks mitigates the impact of white matter lesions in the elderly. Alzheimer's research & therapy 10 (1), 109.

Bethlehem, R.A., Paquola, C., Seidlitz, J., Ronan, L., Bernhardt, B., Tsvetanov, K.A., Cam-CAN, Consortium, 2020. Dispersion of functional gradients across the adult lifespan. NeuroImage 222, 117299.

Betzel, R.F., Byrge, L., He, Y., Goñi, J., Zuo, X.N., Sporns, O., 2014. Changes in structural and functional connectivity among resting-state networks across the human lifespan. Neuroimage 102, 345–357. doi:10.1016/j.neuroimage.2014.07.067.

Black, S., Gao, F., Bilbao, J., 2009. Understanding white matter disease: imaging pathological correlations in vascular cognitive impairment. Stroke 40 (3 Suppl), S48–S52. doi:10.1161/STROKEAHA.108.537704.

Bullmore, E., Sporns, O., 2009. Complex brain networks: graph theoretical analysis of structural and functional systems. Nat. rev. neurosci. 10 (3), 186. doi:10.1038/nrn2575.

Cassel, C., Hackl, P., Westlund, A.H., 1999. Robustness of partial least-squares method for estimating latent variable quality structures. J. applied statistics 26 (4), 435–446.

Chan, M.Y., Park, D.C., Savalia, N.K., Petersen, S.E., Wig, G.S., 2014. Decreased segregation of brain systems across the healthy adult lifespan. Proc. Natl. Acad. Sci. USA., 111 (46), E4997–E5006. doi:10.1073/pnas.1415122111.

Chong, M., Bhushan, C., Joshi, A.A., Choi, S1, Haldar, J.P., Shattuck, D.W., Spreng, R.N., Leahy, R.M., 2017. Individual Parcellation of resting fMRI with a group functional connectivity prior. NeuroImage 156, 87–100. doi:10.1016/j.neuroimage.2017.04.054.

Cook, I.A., Leuchter, A.F., Morgan, M.L., Dunkin, J.J., Witte, E., David, S., Mickes, L., O'Hara, R., Simon, S., Lufkin, R., Abrams, M., Rosenberg, S., 2004. Longitudinal progression of subclinical structural brain disease in normal aging. Am. J. Geriatr. Psychiatry. 12 (2), 190–200. doi:10.1097/00019442200403000-00010.

Damoiseaux, J.S., 2017. Effects of aging on functional and structural brain connectivity. Neuroimage 160, 32–40. doi:10.1016/j.neuroimage.2017.01.077.

Davis, S.W., Dennis, N.A., Daselaar, S.M., Fleck, M.S., Cabeza, R., 2008. Que PASA? The posterior–anterior shift in aging. Cerebral cortex 18 (5), 1201–1209.

Debette, S., Markus, H.S., 2010. The clinical importance of white matter hyperintensities on brain magnetic resonance imaging: systematic review and metaanalysis. BMJ 341, c3666. doi:10.1136/bmj.c3666.

De Leeuw, F.E., de Groot, J.C., Achten, E., Oudkerk, M., Ramos, L.M.P., Heijboer, R., Hofman, A., Jolles, J., van Gijn, J., Breteler, M.M., 2001. Prevalence of cerebral white matter lesions in elderly people: a population based magnetic resonance imaging study. The Rotterdam Scan Study. J Neurol Neurosurg Psychiatry 70 (1), 9–14. doi:10.1136/jnnp.70.1.2.

De Leeuw, F.E., de Groot, J.C., Oudkerk, M., Witteman, J.C., Hofman, A., van, G.J., et al., 2002. Hypertension and cerebral white matter lesions in a prospective cohort study. Brain 125, 765–772.

De Marco, M., Manca, R., Mitolo, M., Venneri, A., 2017. White matter hyperintensity load modulates brain morphometry and brain connectivity in healthy adults: a neuroplastic mechanism? Neural plasticity 2017. doi:10.1155/2017/4050536.

Dey, A.K., Stamenova, V., Turner, G., Black, S.E., Levine, V., 2016. Pathoconnectomics of cognitive impairment in small vessel disease: A systematic review. Alzheimer's & dementia : the journal of the Alzheimer's Association 12 (7), 831–845.

Efron, B, Tibshirani, R, 1986. Bootstrap methods for standard errors, confidence intervals and other measures of statistical accuracy. Stat. Sci. 1, 54–77.

Esiri, M.M., 2007. Ageing and the brain. J. Pathol. 211 (2), 181–187.

Feng, C., Wang, H., Lu, N., Chen, T., He, E., Lu, Y, 2014. Log-transformation and its implications for data analysis. Shanghai archives of psychiatry 26 (2), 105.

Fischl, B., 2012. FreeSurfer. NeuroImage 62 (2), 774–781. doi:10.1016/j.neuroimage.2012.01.021.

Folstein, M.F., Folstein, S.E., McHugh, P.R., 1975. Mini-Mental State" A practical method for grading the cognitive state of patients for the clinician. J. Psychiatric Res. 12, 189–198. doi:10.1016/0022-3956(75)90026-6.

Fox, M.D., Raichle, M.E., 2007. Spontaneous fluctuations in brain activity observed with functional magnetic resonance imaging. Nature rev. neurosci. 8 (9), 700–711.

Fridriksson, J., Guo, D., Fillmore, P., Holland, A., Rorden, C., 2013. Damage to the anterior arcuate fasciculus predicts non-fluent speech production in aphasia. Brain 136. doi:10.1093/brain/awt267, 3451e3460.

Gazzaley, A., Cooney, J.W., Rissman, J., D'Esposito, M, 2005. Top-down suppression deficit underlies working memory impairment in normal aging. Nat. Neurosci. 8 (10), 1298–1300. doi:10.1038/nn1543.

Ge, T., Holmes, A.J., Buckner, R.L., Smoller, J.W., Sabuncu, M.R., 2017. Heritability analysis with repeat measurements and its application to resting-state functional connectivity. Pro. Natl. Acad. Sci. U.S.A. 114 (21), 5521–5526. doi:10.1073/pnas.1700765114.

Geerligs, L., Renken, R.J., Saliasi, E., Maurits, N.M., Lorist, M.M., 2015. A brain-wide study of age-related changes in functional connectivity. Cerebral cortex 25 (7), 1987–1999.

Gershon, R.C., Wagster, M.V., Hendrie, H.C., Fox, N.A., Cook, K.F., Nowinski, C.J., 2013. NIH toolbox for assessment of neurological and behavioral function. Neurology 80 (11 Suppl 3), S2–S6.

Ghasemi, A., Zahediasl, S., 2012. Normality tests for statistical analysis: a guide for non-statisticians. Int. j. endocrinol. and metabolism 10 (2), 486.

Greve, D.N., Fischl, B., 2009. Accurate and robust brain image alignment using boundary-based registration. NeuroImage 48 (1), 63–72. doi:10.1016/j.neuroimage.2009.06.060.

Griebe, M., Amann, M., Hirsch, J.G., Achtnichts, L., Hennerici, M.G., Gass, A., Szabo, K, 2014. Reduced functional reserve in patients with age-related white matter changes: a preliminary fMRI study of working memory. PLoS One 9, e103359. doi:10.1371/journal.pone.0103359.

Gunning-Dixon, F.M., Raz, N., 2000. The cognitive correlates of white matter abnormalities in normal aging: a quantitative review. Neuropsychology 14 (2), 224.

Habes, M, Erus, G, Toledo, JB, Bryan, N, Janowitz, D, Doshi, J, et al., 2018. Regional tract-specific white matter hyperintensities are associated with patterns to aging-related brain atrophy via vascular risk factors, but also independently. Alzheimers Dement. 10, 278–284.

Johnston, J.M., Vaishnavi, S.N., Smyth, M.D., Zhang, D., He, B.J., Zempel, J.M., Shimony, J.S., Snyder, A.Z., Raichle, M.E., 2008. Loss of resting interhemispheric functional connectivity after complete section of the corpus callosum. J. Neurosci 28. doi:10.1523/JNEUROSCI.0573-08.2008, 6453e6458.

Kennedy, K.M., Raz, N., 2015. Normal aging of the brain. In: Toga, A.W. (Ed.), Brain Mapping: an Encyclopedic Reference. Elsevier.

Kloppenborg, R.P., Nederkoorn, P.J., Geerlings, M.I., van den Berg, E., 2014. Presence and progression of white matter hyperintensities and cognition: a meta-analysis. Neurology 82 (23), 2127–2138.

Kramer, J.H., Mungas, D., Reed, B.R., Wetzel, M.E., Burnett, M.M., Miller, B.L., Weiner, M.W., Chui, H.C., 2007. Longitudinal MRI and cognitive change in healthy elderly. Neuropsychology 21 (4), 412.

Kundu, P., Benson, B.E., Rosen, D., Frangou, S., Leibenluft, E., Luh, W.M., Bandettini, P.A., Pine, D.S., Ernst, M., 2018. The integration of functional brain activity from adolescence to adulthood. J. Neurosci 38 (14), 3559–3570.

Kundu, P., Brenowitz, N.D., Voon, V., Worbe, Y., Vértes, P.E., Inati, S.J., Saadd, S., Bandettini, P.A., Bullmore, E.T., 2013. Integrated strategy for improving functional connectivity mapping using multiecho fMRI. Proc. Natl. Acad. Sci. U S A. 110 (40), 16187–16192. doi:10.1073/pnas.1301725110.

Kundu, P., Inati, S.J., Evans, J.W., Luh, W.M., Bandettini, P.A., 2012. Differentiating BOLD and non-BOLD signals in fMRI time series using multi-echo EPI. Neuroimage 60 (3), 1759–1770. doi:10.1016/j.neuroimage.2011.12.028.

Kundu, P., Voon, V., Balchandani, P., Lombardo, M.V., Poser, B.A., Bandettini, P.A., 2017. Multi-echo fMRI: a review of applications in fMRI denoising and analysis of BOLD signals. Neuroimage 154, 59–80.

Langen, C.D., Zonneveld, H.I., White, T., Huizinga, W., Cremers, L.G., de Groot, M., Ikram, M.A., Niessen, W.J., Vernooij, M.W., 2017. White matter lesions relate to tract-specific reductions in functional connectivity. Neurobiol. Aging 51, 97–103. doi:10.1016/j.neurobiolaging.2016.12.004.

Kong, R., Yang, Q., Gordon, E., Xue, A., Zho, X, Spreng, R.N., Ge, T., Holmes, A.J., Eickhoff, S., Yeo, B.T.T., 2021. Individual-specific areal-level parcellations improve functional connectivity prediction of behavior. Cerebral Cortex 31, 4477–4500.

Malagurski, B., Liem, F., Oschwald, J., Mérillat, S., Jäncke, L., 2020. Functional dedifferentiation of associative resting state networks in older adults–A longitudinal study. NeuroImage 214, 116680.

McIntosh, A.R., Lobaugh, N.J., 2004. Partial least squares analysis of neuroimaging data: applications and advances. NeuroImage 23, S250–S263. doi:10.1016/j.neuroimage.2004.07.020.

McIntosh, A.R., Mišić, B., 2013. Multivariate statistical analyses for neuroimaging data. Annu Rev Psychol 64 (1), 499–525. doi:10.1146/annurev- psych-113011-143804.

Mwilambwe-Tshilobo, L., Ge, T., Chong, M., Ferguson, M.A., Misic, B., Burrow, A.L., Leahy, R.M., Spreng, R.N., 2019. Loneliness and meaning in life are reflected in the intrinsic network architecture of the brain. Soc Cogn Affect Neurosci 14 (4), 423–433. doi:10.1093/scan/nsz021.

Ng, K.K., Lo, J.C., Lim, J.K., Chee, M.W., Zhou, J., 2016. Reduced functional segregation between the default mode network and the executive control network in healthy older adults: A longitudinal study. NeuroImage 133, 321–330.

Nomura, E.M., Gratton, C., Visser, R.M., Kayser, A., D'Esposito, F., 2010. Double dissociation of two cognitive control networks in patients with focal brain lesions. Proc Natl Acad Sci U S A 107 (26).

Power, J.D., Barnes, K.A., Snyder, A.Z., Schlaggar, B.L., Petersen, S.E., 2012. Spurious but systematic correlations in functional connectivity MRI networks arise from subject motion. NeuroImage 59 (3), 2142–2154. doi:10.1016/j.neuroimage.2011.10.018.

Power, J.D., Plitt, M., Gotts, S.J., Kundu, P., Voon, V., Bandettini, P.A., Martin, A., 2018. Ridding fMRI data of motion-related influences: Removal of signals with distinct spatial and physical bases in multiecho data. Proceedings of the National Acad. Sci. 115 (9), E2105–E2114.

Prins, N.D., Scheltens, P., 2015. White matter hyperintensities, cognitive impairment and dementia: an update. Nature Rev. Neurol. 11 (3), 157–165.

Quandt, F., Fischer, F., Schröder, J., Heinze, M., Lettow, I., Frey, B.M., Gerloff, C., 2020. Higher white matter hyperintensity lesion load is associated with reduced long-range functional connectivity. Brain comm. 2 (2), fcaa111.

Raz, N., Lindenberger, U., Rodrigue, K.M., Kennedy, K.M., Head, D., Williamson, A., Dahle, C., Gerstorf, D., Acker, J.D., 2005. Regional brain changes in aging healthy adults: general trends, individual differences and modifiers. Cereb Cortex 15 (11), 1676–1689. doi:10.1093/cercor/bhi044.

Resnick, S.M., Pham, D.L., Kraut, M.A., Zonderman, A.B., Davatzikos, C., 2003. Longitudinal magnetic resonance imaging studies of older adults: a shrinking brain. Journal of Neuroscience 23 (8), 3295–3301.

Reuter-Lorenz, Cappell, K.A, 2008. Neurocognitive aging and the compensation hypothesis. Curr Dir Psychol Sci 17 (3), 177–182. doi:10.1111/j.1467-8721.2008.00570.x.

Sachdev, P., Kalaria, R., O'Brien, J., Skoog, I., Alladi, S., Black, S.E., Scheltens, P., 2014. Diagnostic criteria for vascular cognitive disorders: a VASCOG statement. Alzheimer dis. and associated disorders 28 (3), 206.

Sbardella, E., Petsas, N., Tona, F., Pantano, P., 2015. Resting-state fMRI in MS: general concepts and brief overview of its application. BioMed res. Int. 2015, 212693.

Schaefer, A., Kong, R., Gordon, E., Laumann, T.O., Zuo, X.N., Holmes, A.J., Eickhoff, S.B., Yeo, B.T.T., 2018. Local-Global Parcellation of the Human Cerebral Cortex from Intrinsic Functional Connectivity MRI. Cereb Cortex 28 (9), 3095–3114. doi:10.1093/cercor/bhx179.

Schmidt, P., Gaser, C., Arsic, M., Buck, D., Förschler, A., Berthele, A., Hoshi, M., Ilg, R., Schmid, V.J., Zimmer, C., Hemmer, B., Mühlau, M., 2012. An automated tool for detection of FLAIR-hyperintense white-matter lesions in multiple sclerosis. Neuroimage 59 (4), 3774–3783. doi:10.1016/j.neuroimage.2011.11.032.

Schmidt, P., Mühlau, M., Gaser, C., & Wink, L. (2013). LST: A lesion segmentation tool for SPM.

Schonberg, T., Pianka, P., Hendler, T., Pasternak, O., Assaf, Y., 2006. Characterization of displaced white matter by brain tumors using combined DTI and fMRI. Neuroimage 30, 1100–1111. doi:10.1016/j.neuroimage.2005.11.015.

Seghier, M.L., Lazeyras, F., Zimine, S., Maier, S.E., Hanquinet, S., Delavelle, J., Volpe, J.J., Huppi, P.S., 2004. Combination of event-related fMRI and diffusion tensor imaging in an infant with perinatal stroke. Neuroimage 21, 463–472.

Setton, R., Mwilambwe-Tshilobo, L., Girn, M., Lockrow, A.W., Baracchini, G., Lowe, A.J., Cassidy, B.N., Li, J., Luh, W.-M., Bzdok, D., Leahy, R.M., Ge, T., Marguilies, D.S., Mišić, B., Bernhardt, B.C., Stevens, W.D., De Brigard, F., Kundu, P., Turner, G.R., Spreng, R.N, 2022. Functional architecture of the aging brain. Cerebral Cortex doi:10.1093/cercor/bhac056, In press.

Shafiei, G., Zeighami, Y., Clark, C.A., Coull, J.T, Nagano-Saito, A., Leyton, M., Dagher, A., Mišic, B., 2019. Dopamine Signaling modulates the stability and integration of intrinsic brain networks. Cereb Cortex 29 (1), 397–409. doi:10.1093/cercor/bhy264.

Snowdon, D.A., Greiner, L.H., Mortimer, J.A., Riley, K.P., Greiner, P.A., Markesbery, W.R., 1997. Brain infarction and the clinical expression of Alzheimer disease: the Nun Study. Jama 277 (10), 813–817.

Soares, J.M., Conde, R., Magalhães, R., Marques, P., Magalhães, R., Gomes, L., Sampaio, A., 2021. Alterations in functional connectivity are associated with white matter lesions and information processing efficiency in multiple sclerosis. Brain imaging and behave. 15 (1), 375–388.

Song, J., Young, B.M., Nigogosyan, Z., Walton, L.M., Nair, V a, Grogan, S.W., Tyler, M.E., Farrar-Edwards, D., Caldera, K.E., Sattin, J.A., Williams, J.C., Prabhakaran, V., 2014. Characterizing relationships of DTI, fMRI, and motor recovery in stroke rehabilitation utilizing brain-computer interface technology. Front. Neuroeng 7, 31. doi:10.3389/fneng.2014.00031.

Speck, O., Ernst, T., Chang, L., 2001. Biexponential modeling of multigradient-echo MRI data of the brain. Magnetic Resonance in Med.: An Off. J. Int. Soc. for Magnetic Resonance in Med. 45 (6), 1116–1121.

Spreng, R.N., Fernández-Cabello, S., Turner, G.R., Stevens, W.D., 2019. Take a deep breath: Multiecho fMRI denoising effectively removes head motion artifacts, obviating the need for global signal regression. Proceedings of the National Acad. Sci. 116 (39), 19241–19242.

Spreng, R.N., Turner, G.R., 2019b. Structure and function of the aging brain. In: Samanez-Larkin, G. (Ed.), The Aging Brain. American Psychological Association, Washington DC.

Staffaroni, A.M., Brown, J.A., Casaletto, K.B., Elahi, F.M., Deng, J., Neuhaus, J., Cobigo, Y., Mumford, P.S, Walters, S., Saloner, R., Karydas, A., Coppola, G., Rosen, H.J., Miller, B.L., Seeley, W.W., Kramer, J.H., 2018. The Longitudinal Trajectory of Default Mode Network Connectivity in Healthy Older Adults Varies As a Function of Age and Is Associated with Changes in Episodic Memory and Processing Speed. J Neurosci 38 (11), 2809–2817.

Stevens, W.D., Spreng, R.N., 2014. Resting-state functional connectivity MRI reveals active processes central to cognition. Wiley International Reviews (WIREs) Cognitive Science 5, 233–245.

Stumme, J., Jockwitz, C., Hoffstaedter, F., Amunts, K., Caspers, S., 2020. Functional network reorganization in older adults: Graph-theoretical analyses of age, cognition and sex. NeuroImage 214, 116756.

Turner, G.R., D'Esposito, M, 2010. Functional neuroimaging in aging. In: Knoefel, J., Albert, M. (Eds.), Clinical Neurology of Aging, 3rd Edition. Oxford University Press, New York.

Vasquez, B.P., Zakzanis, K.K., 2015. The neuropsychological profile of vascular cognitive impairment not demented: a meta-analysis. J. Neuropsychol. 9 (1), 109–136.

Varangis, E., Habeck, C.G., Razlighi, Q.R., Stern, Y., 2019. The effect of aging on resting state connectivity of predefined networks in the brain. Frontiers in aging neurosci. 11, 234.

Vernooij, M.W., Ikram, M.A., Tanghe, H.L., Vincent, A.J., Hofman, A., Krestin, G.P., Niessen, W.J., Breteler, M.M., van der Lugt, A., 2007. Incidental findings on brain MRI in the general population. N Eng J Med 357 (18), 1821–1828. doi:10.1056/NEJMoa070972.

Walsh, P., Sudre, C.H., Fiford, C.M., Ryan, N.S., Lashley, T., Frost, C., Barnes, J.ADNI Investigators, 2020. CSF amyloid is a consistent predictor of white matter hyperintensities across the disease course from aging to Alzheimer's disease. Neurobiol. aging 91, 5–14.

Wirth, M., Villeneuve, S., Haase, C.M., Madison, C.M., Oh, H., Landau, S.M., Jagust, W.J., 2013. Associations between Alzheimer disease biomarkers, neurodegeneration, and cognition in cognitively normal older people. JAMA neurol. 70 (12), 1512–1519.

World health statistics 2021: monitoring health for the SDGs, sustainable development goals. World Health Organization. Geneva. Licence: CC BY-NC-SA 3.0 IGO.

Yarchoan, M., Xie, S.X., Kling, M.A., Toledo, J.B., Wolk, D.A., Lee, E.B., Van Deerlin, V., Lee, V.M., Trojanowski, J.Q., Arnold, S.E, 2012. Cerebrovascular atherosclerosis correlates with Alzheimer pathology in neurodegenerative dementias. Brain 135, 3749–3756.

Yang, Z., Wen, W., Jiang, J., Crawford, J.D., Reppermund, S., Levitan, C., Slavin, M.J., Kochan, N.A., Richmond, R.L., Brodaty, H., et al., 2016. Age-associated differences on structural brain MRI in nondemented individuals from 71 to 103 years. Neurobiol. Aging 40, 86–97.

Yeo, B.T., Krienen, F.M., Sepulcre, J., Sabuncu, M.R., Lashkari, D., Hollinshead, M., Roffman, J.L., Smoller, J.W., Zöllei, L., Polimeni, J.R., Fischl, B., Liu, H., Buckner, R.L., 2011. The organization of the human cerebral cortex estimated by intrinsic functional connectivity. J Neurophysiol 106 (3), 1125–1165. doi:10.1152/jn.00338.2011.

Yesavage, J.A., Brink, T.L., Rose, T.L., Lum, O., Huang, V., Adey, M., Leirer, V.O., 1982. Development and validation of a geriatric depression screening scale: a preliminary report. J. Psychiatr. Res. 17 (1), 37–49.

Xia, M., Wang, J., He, Y., 2013. BrainNet viewer: a network visualization tool for human brain Connectomics. PLoS One 8 (7), e68910. doi:10.1371/journal.pone.0068910.

Zhou, B., Yao, H., Wang, P., Zhang, Z., Zhan, Y., Ma, J., Zhang, X., 2015. Aberrant functional connectivity architecture in Alzheimer's disease and mild cognitive impairment: a whole-brain, data-driven analysis. BioMed res. Int. 2015, 495375.